Origin of nonlinear sputtering during nanocluster bombardment of metals

Juha Samela* and Kai Nordlund
Accelerator Laboratory, University of Helsinki, P.O. Box 43, FIN-00014 Espoo, Finland
(Received 31 May 2007; revised manuscript received 31 July 2007; published 28 September 2007)

Recent experiments [S. Bouneau *et al.*, Phys. Rev. B **65**, 144106 (2002)] show that the sputtering of atoms from surfaces by cluster impacts behaves differently from what is expected in the classical stopping theory. The most significant unresolved questions are that the sputtering yield divided by cluster nuclearity squared (Y/N^2) is independent of N in the size range $N=2-13$ and that the energy maximum is not at the position expected from the nuclear stopping power. We use classical molecular dynamics simulations to examine the energy deposition from 0.1–18.5 MeV Au_5 and Au_{13} clusters to the Au(111) surface to investigate this question. The simulations show that only a portion of the energy deposited from the cluster atoms to the crystal contributes to the formation of the displacement cascade because either the cluster channels through the surface layers as one entity or, if strong collisions occur, the energy deposited in these collisions is mostly carried away from the collision region by fast knock-on atoms. Based on the observations in the simulations, we develop an analytical model that explains the N^2 effect and an energy maximum that differs from the nuclear stopping.

DOI: 10.1103/PhysRevB.76.125434 PACS number(s): 61.80.Az, 36.40.Qv, 61.46.Bc, 61.80.Jh

I. INTRODUCTION

Ion and atomic cluster beams are used widely in industry to smooth surfaces and eject material for coating and layer deposition.[1] The ejection of material, usually called sputtering, is well understood at low energies and when atomic ion beams are used. Sigmund and Clausen published already in 1981 a model which describes collisions of heavy atom or molecular ions on metals and predicts sputtering yields.[2] However, the model does not explain the recent experimental findings concerning sputtering induced by nanocluster beams.[3]

The sputtering yield of nanocluster bombardment is nonlinear with cluster size. The yield is remarkably larger than the sum of yields induced by the constituent cluster atoms, if they arrived separately with the same kinetic energy.[4–6] In addition, the ratio Y/N^2, where Y is the average sputtering yield per cluster and N is the nuclearity of clusters (number of atoms in a cluster), is independent of nuclearity in a fairly wide range of cluster sizes and energies.[6] This so-called N^2 effect is not yet explained, in addition to some other phenomena in 50–300 keV/atom Au_n cluster bombardment.[7] Moreover, the energy maximum of the sputtering yield is not at the position expected from the nuclear stopping power. Attempts have been made to explain these effects using atomistic computer simulations,[8–10] but the simulations run, until now, have not reached sufficiently high energies to examine the effects around the energy maximum. Large craters, large defects, and sputtered clusters are also observed in cluster bombardment simulations.[11,12]

The mechanism of nanocluster bombardment is not only an interesting scientific problem but has also a great value from an application point of view. Tailored applications of cluster beams could be developed more easily on the basis of better understanding of collision mechanisms. Resistance to high-energy bombardment is also important for fusion reactor materials.

In the present work, we use classical molecular dynamics simulations to examine the energy deposition from 0.1–18.5 MeV Au_5 and Au_{13} clusters to the Au(111) surface. Based on the simulations, we introduce a simple model called the *droplet model*. It combines several atomic level processes to an analytical framework that provides an explanation to the N^2 behavior of the sputtering yield and the maximum in energy. According to the droplet model, the energy dependence of the sputtering yield can be predicted by assuming that the cluster first penetrates a certain distance inside the solid as one entity and then gradually falls apart forming a spherical or ellipsoidal collision cascade. The model breaks the complicated problem of cluster collisions into smaller parts, which may be solved separately in order to develop a comprehensive theory of cluster collisions in the future.

II. METHODS

In cluster impacts, the sputtered target atoms come mostly from the surface layers of the crystal, and the sputtering yield is often directly proportional to the area of the crater induced by the impact.[13] The size of the crater is, in turn, proportional to the size of the displacement cascade, which is a region of high-energy target atoms displaced at least 2.5 Å from their initial positions. The primary cause for the cascade formation is the energy deposited from the cluster atoms when they either stop in the surface layer or move through it colliding with the target atoms. According to the simulations, this energy deposition to the surface layers lasts only 10–100 fs depending on the cluster energy. To find out the energy deposition mechanisms, we simulated these very early phases of impacts.

In the simulations, a Au(111) surface was bombarded with Au_5 and Au_{13} cluster at energies 20–1500 keV/atom. Although most of the experimental sputtering data are from polycrystalline targets, the Au(111) crystal was chosen to investigate the basic energy deposition mechanisms without effects of grain boundaries and various crystal orientations.

The angle of incidence was 0° in the Au_{13} simulations and 0° or 6° in the Au_5 simulations. The impact point on the

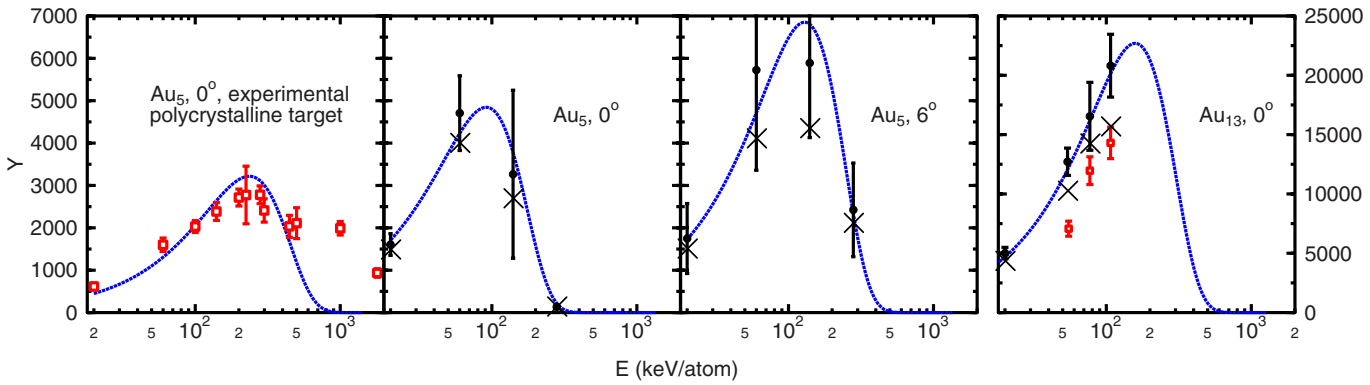

FIG. 1. (Color online) Experimental (Ref. 6) and simulated total sputtering yields as function of cluster energy (keV/atom). The experimental Au_5 yields are shown in the left frame, and all three experimental Au_{13} yield points available in Ref. 6 are plotted in the right frame (squares). The Au_5 yields in the middle frames are simulated with 0° and 6° angles of incidence and the Au_{13} yield in the right frame with 0°. The simulated yields are averages of three runs and the errors are standard deviations. The initial yields just after the sputtering has stopped are marked with circles, and the final yields after the fragmentation of sputtered clusters are marked with crosses. The blue lines show fittings of Eq. (4) to the data with parameters given in Table I.

surface as well as the spatial orientation of the cluster were varied randomly between the simulation runs. At each energy and angle, a series of 32 simulations was run to get reliable averages. The target lattice was 7 nm wide and 14 nm deep, which is large enough to ensure that the reflected shock waves do not disturb the impact area during the first 30–100 fs simulations. Position, energies, velocities, and accelerations were detected every femtosecond.

When a cluster atom moves through the Au(111) crystal to the [111] direction, most of the collisions during the first femtoseconds occur with target atoms in the untouched crystal planes. Even when the cluster atom goes perpendicularly through a crystal plane, usually more than one atom in the plane interacts simultaneously with the cluster atom and the collision dynamics cannot be reduced to a series of binary collisions. Therefore, in the analysis presented in the following sections, the energy loss of a cluster atom in one Au(111) unit cell is considered a collision. In other words, the energy loss of the cluster atoms is calculated in each 7.0636 Å unit cell layer. This level of accuracy is enough for calculation of the average quantities for the purposes of this study.

In addition to the first femtosecond simulations, the sputtering yields were calculated in 100–140 ps large-scale simulations. The size of the crystal lattice in these simulations was $49\times49\times50$ nm^3 containing almost 7×10^6 atoms, which ensured that the simulated cascades were not distorted by artificial boundaries. Because of the large number of atoms, each simulation run took several thousand hours of computer time. This limited the number of cluster and energy variations. The energies up to 280 keV/atom were possible in practice.

Electronic stopping is an important energy loss mechanism at the energies studied in the simulations. Therefore, electronic stopping was applied as a nonlocal frictional force to all atoms having a kinetic energy larger than 5 eV.[14,15] Because the energy lost by this mechanism is removed from the system, it does not change the motion of the other atoms. A consequence is that both nuclear and electronic energy losses are included in the analysis of deposited energy, but the electronic energy loss does not contribute to the cascade formation in the simulations except the fact that it slows down the channeling atoms. Duvenbeck *et al.*[16] have recently shown that the energy absorbed by electrons can affect sputtering in Ag, but the kinetic energy at the surface is always considerably higher than the excitation energy of the electron gas, which justifies our approximation that only the energy deposited by the nuclear stopping contributes to the cascade formation.

The potential used in this study is based on the corrected effective medium (CEM) theory.[17,18] The target and the clusters were stabilized using this potential before the impact simulations. Spherical clusters were used. According to *ab initio* calculations, planar Au cluster structures are energetically favorable up to $N=13$,[19] whereas with the CEM potential, the stable Au_{13} structure is icosahedral. However, our test simulations with planar Au_5 clusters show that the cluster shape does not affect the shapes of the collision cascades significantly at energies high enough to produce large craters. The ambient temperature for all simulations was 100 K. Other details of the simulation method are described in Refs. 13 and 20–22.

III. RESULTS

A. Total sputtering yields

The simulated Au_5 sputtering yields plotted as function of the cluster energy are similar in shape as the experimental Au_5 yields[6] as shown in Fig. 1. In both cases, the maximum yield is reached at very low energies compared to the maximum of the nuclear stopping ($\approx$700 keV),[14] which rules out the most simple explanation that the yields begin to decrease with nuclear stopping.

The final sputtering yields are lower than the initial yields calculated immediately after the sputtering has stopped, because of the fragmentation of large sputtered clusters and the consequent return of material back to the surface.[12,23,24] In general, the fragmentation is more important for large yields, which usually contain large sputtered clusters initially.[13] This effect is taken into consideration by simulating the sputtered

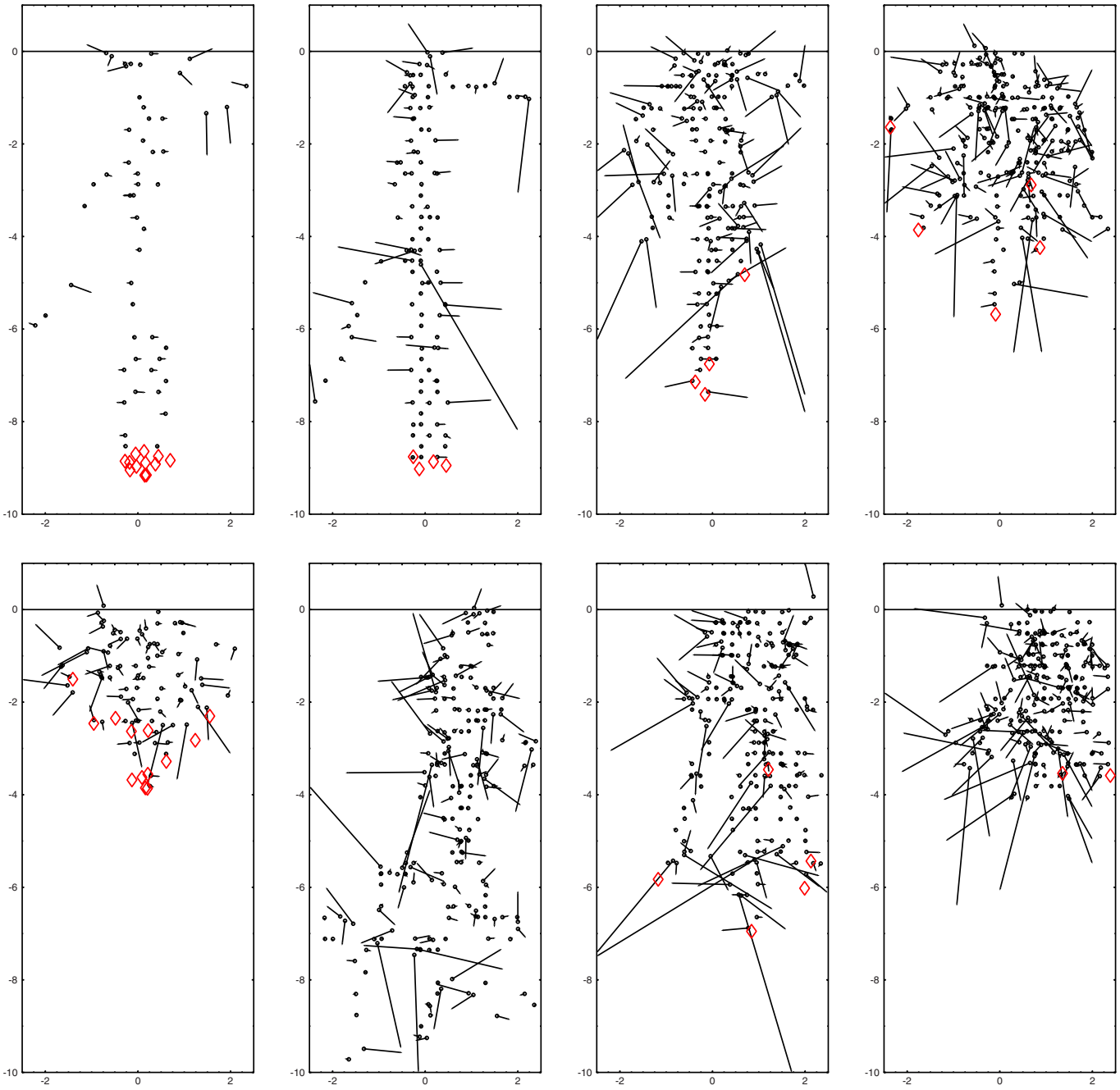

FIG. 2. (Color online) Visualizations of velocities induced by different events. Top row: 1500 keV Au_{13}, 0°; 1000 keV Au_5, 0°; 140 keV Au_5, 0°; and 60 keV Au_5, 0°. Bottom row: 77 keV Au_{13}, 0°; 1000 keV Au_5, 6°; 140 keV Au_5, 6°; and 60 keV Au_5, 6°. Only atoms moving faster than 100 km/s are shown. The arrows are relative velocities on the plane. It follows that the atoms with small arrows may have considerable velocity perpendicular to the plane. Cluster atoms are marked with diamond (red in the online version). Snapshots are taken 15–40 fs after the impact depending on energy. Au_{13} results are from Ref. 13.

material an additional 3–10 ns until the yield is stabilized. The simulated final yields are marked with crosses in Fig. 1 for comparison to the experimental values.

The Au_{13} yields are in good agreement with the experimental values, whereas the Au_5 yields show only a qualitatively similar energy dependence. The experimental yield reaches its maximum at around 300 keV, which is considerably higher than the maxima found in the simulations. The difference between initial and final yields does not explain the disagreement. The experimental yields are measured from a polycrystalline target, whereas in the simulations, we have used a perfect Au(111) target to simplify the analysis of effective factors. As we will show, the channeling decreases the sputtering yield at high energies. Therefore, the most obvious explanation to the disagreement is that the channeling of the cluster atoms is more probable in the simulations than in the polycrystalline target used in the experiment. In addition, the surface roughness of the real target may increase the yield. The dependence of the sputtering yield on the structure of the target is experimentally demonstrated in

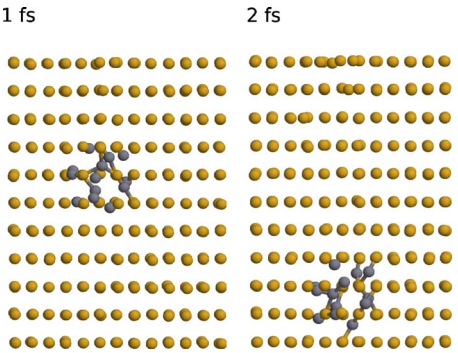

FIG. 3. (Color online) A 1500 keV/atom Au_{13} cluster penetrating into to the Au(111) crystal. The rightmost frame shows disorder in the same region after 55 fs.

nanodispersed gold targets by Baranov *et al.*[25] At the moment, it is not possible in practice to simulate large enough polycrystalline targets to directly compare the experimental and simulated yields at energies higher than 280 keV.

B. Collision types

Before analysis of statistical quantities, let us first discuss the overall chain of events using some typical single impacts as examples. In spite of the statistical variations between impacts, common features can be easily found in a set of events.

Figure 2 shows that both 1500 keV/atom Au_{13} and 1000 keV/atom Au_5 clusters channel through the surface layer of the crystal very effectively when they arrive at zero angle. Single atoms can depart from the others and end up in a channel not parallel to its original channel. Also, some primary knock-on atoms move fast in channels perpendicular to the cluster track. The 140 keV/atom cluster falls apart in the surface layer, although its atoms channel separately deeper into the crystal. Destruction of the 60 keV/atom cluster in the surface layer is complete. It deposits all of its energy near the surface.

The atoms in the channel walls gain momenta perpendicular to the channel as shown in Fig. 2. According to the binary collision theory, this is what should happen because the impact parameter is usually large in the collisions between channeling atoms and channel wall atoms. The rightmost frame in Fig. 3 shows that the atoms in the crystal planes are here and there packed tightly, probably because of the pressure induced by these collisions. This response is partly elastic and decreases the probability of crystal destruction and displacement cascade formation.

In general, the atoms of low-energy clusters undergo many small collisions in the surface layer, which destroys the crystal structure effectively over a large region. The cascade opens the surface and its content is released to vacuum, giving a high sputtering yield.[13] The high-energy clusters either channel through the surface layer or deposit their energy in a few violent collisions. However, these collisions do not usually occur near each other, and the high-energy knock-on atoms spread the energy over a large volume. So, no large displacement cascade is formed and the yield is small at high energies.

The cluster size does not affect this behavior. Figure 3 shows that the atoms of a Au_{13} go in the neighboring channels. The cluster is slightly reshaped when it reaches the surface to avoid direct collisions to the crystal atoms in the first layer. After that, the mutual location of cluster atoms does not change very much when it moves several nanometers in the crystal. In some Au_{13} events, the cluster atom that follows another atom from the same cluster in the same channel undergoes stronger collisions with atoms in the channel walls, because the first atom has disturbed the channel. The atom falls behind the others, and the collisions with wall atoms decelerate the atom even more, until a very violent collision departs the atom from the channel. In general, the cluster atoms depart one by one from the others due to this mechanism, and the cluster energy is deposited over a long range. This is one of the key findings behind the model introduced in Sec. IV.

At 6°, the atoms of the high-energy Au_5 clusters cannot channel easily and they undergo strong collisions with the surface atoms (Fig. 2). The atoms lose their velocity and more energy is deposited in the surface layers than in the normal angle impacts. However, the atoms do not completely stop near the surface but find channels after the strong collisions and continue their way inside the crystal. The most favorable channels for the cluster atoms in Au(111) are those perpendicular to the (111) surface. Also, the low-energy clusters deposit more energy in the surface layers than in the corresponding zero incidence cases.

Ion range calculations based on the Ziegler-Biersack-Littmark (ZBL) potential (MDRANGE software[26]) show that the minimum channeling occurs at 6° angle of incidence for Au(111) surfaces. In general, the channeling of clusters follows the same pattern. This is the main reason to apply the binary collision approximation to this analysis. Most of the primary collisions occur between single cluster atoms and crystal atoms, so the interactions between the cluster atoms do not have a major effect on the energy deposition.

The other crystal orientations introduce differences in channeling probability, but it is probable that the overall behavior of cluster stopping described above will be valid: Channeling increases with energy and changes with angle depending on crystal orientation. Therefore, also the sputtering yields measured from polycrystalline target have the similar energy dependence as the simulated yields from Au(111) (Fig. 1).

C. Energy deposition on the surface layer

High sputtering yields come from dense displacement cascades near the surface[13] induced by the energy deposited in the surface layers. However, the energy loss from cluster atoms at the surface layers cannot directly explain the sputtering yields. Figures 4 and 5 show how the clusters lose energy in the 4.5 nm surface layer. By comparing these results to the yields in Fig. 1, it is clear that a large portion of the deposited energy does not contribute to the cascade formation especially at 4°–6° angles. The 4°–6° impacts have

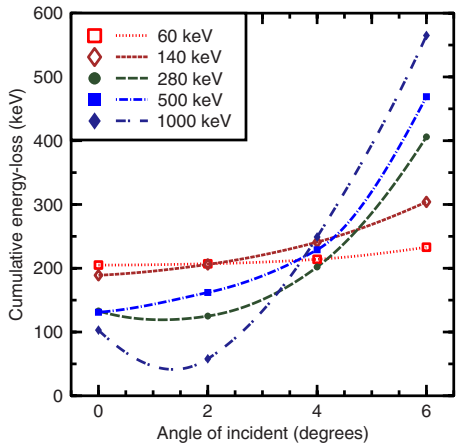

FIG. 4. (Color online) Cluster energy loss in a 0–4.5 nm deep surface layer as function of the cluster's angle of incidence. Each point is the average of 32 Au_5 impacts. The lines are intended as guides for the eye.

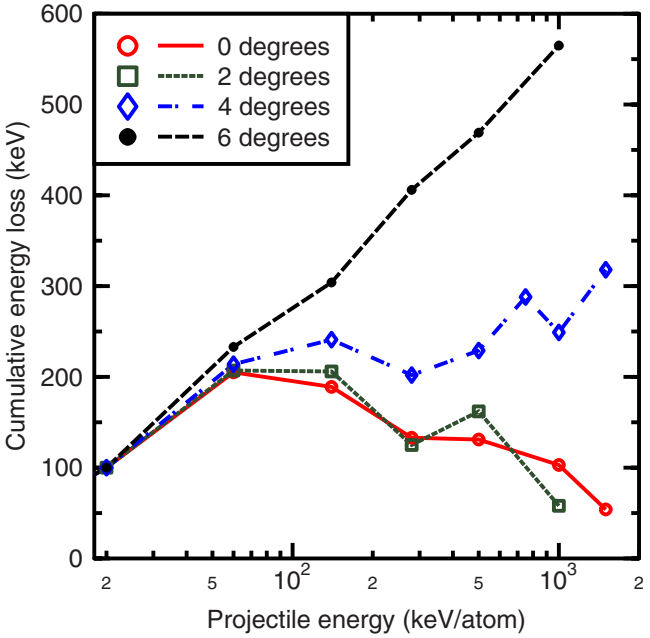

FIG. 5. (Color online) Energy deposited at 0–4.5 nm depth from the surface in Au_5 impacts at various incidence angles. The results are averages of 32 simulations.

more strong collisions, as discussed in the previous section, and therefore, we can conclude that, especially, the energy deposited in these strong collisions does not contribute to the cascade formation.

Figure 4 shows that the angle of incidence does not affect very much on energy deposition at 60 keV/atom, whereas at 1000 keV/atom, the difference is remarkable. This is because the total cluster energy is deposited in the surface layers at low energies regardless of the angle of incidence and because channeling decreases with the angle at high energies. The depth of 4.5 nm was chosen because the simulation indicates that no large surface cascade is formed if the energy is deposited mainly on the deeper layers.

The initial temperature of the target lattice does not considerably affect the energy deposited at the 4.5 nm surface layer at 500–1500 keV/atom. In other words, the atoms are channeled trough the surface layer when the temperature is less than 700 K. Therefore, we conclude that the sputtering yields simulated at 100 K are comparable the experimental values measured at 300 K. However, the energy loss becomes 2–3 times higher at the layers located deeper than 5 nm when the temperature increases from 300 to 700 K. This indicates that the average range of cluster atoms decreases rapidly at high target temperatures, and the shape of the collision cascade is then more spherical.

D. Induced velocities

Two components of momentum induced in the rectangular region around the cluster track are shown in Fig. 6. The vertical component is perpendicular to the surface and has negative values, indicating that the displaced crystal atoms are, in average, moving deeper into the crystal. The horizontal component is the sum of absolute values of all atomic momenta parallel to the surface, regardless of their direction on the plane. Therefore, the horizontal component is always positive and describes mobility parallel to the surface.

Both components of the induced momentum first increase with time and then decrease slowly because momentum is transferred outside the rectangular region. The saturation is reached earlier at high energies because the fast channeling cluster atoms leave the region. At zero angle of incidence, the small energy clusters induce a considerably large momentum than the high-energy clusters, which again leads to the conclusion that channeling decreases cascade formation. At 6° the largest momenta are induced at 280–1000 keV. However, the momenta begin to decrease after 15 fs, indicating that jumps of knock-on atoms transfer momentum outside the track region. Large-scale sputtering simulations are not available above 280 keV/atom, but even the 280 keV/atom yield is small compared to the large momentum induced immediately after the impact.

Figure 7 shows that high-energy collisions are rare compared to collisions of 50 keV/collision or less. However, they deviate the atoms from their route more than the low-energy collisions. In some collisions, the cluster atoms gain energy, which indicates that complicated collision events occur. The gained energy comes from other cluster atoms either directly or transmitted by the crystal atoms. This is visible as a negative energy in Fig. 7.

E. Filtered events

The collisions between cluster and crystal atoms can be classified in three categories. Firstly, the collisions to channel wall atoms do not very much contribute to cascade formation, because the energy deposited is, in most cases, small or it is partly absorbed in the elastic packing of crystal planes, as discussed in Sec. III B. Secondly, the strong collisions of high-energy atoms do not contribute to the cascade formation

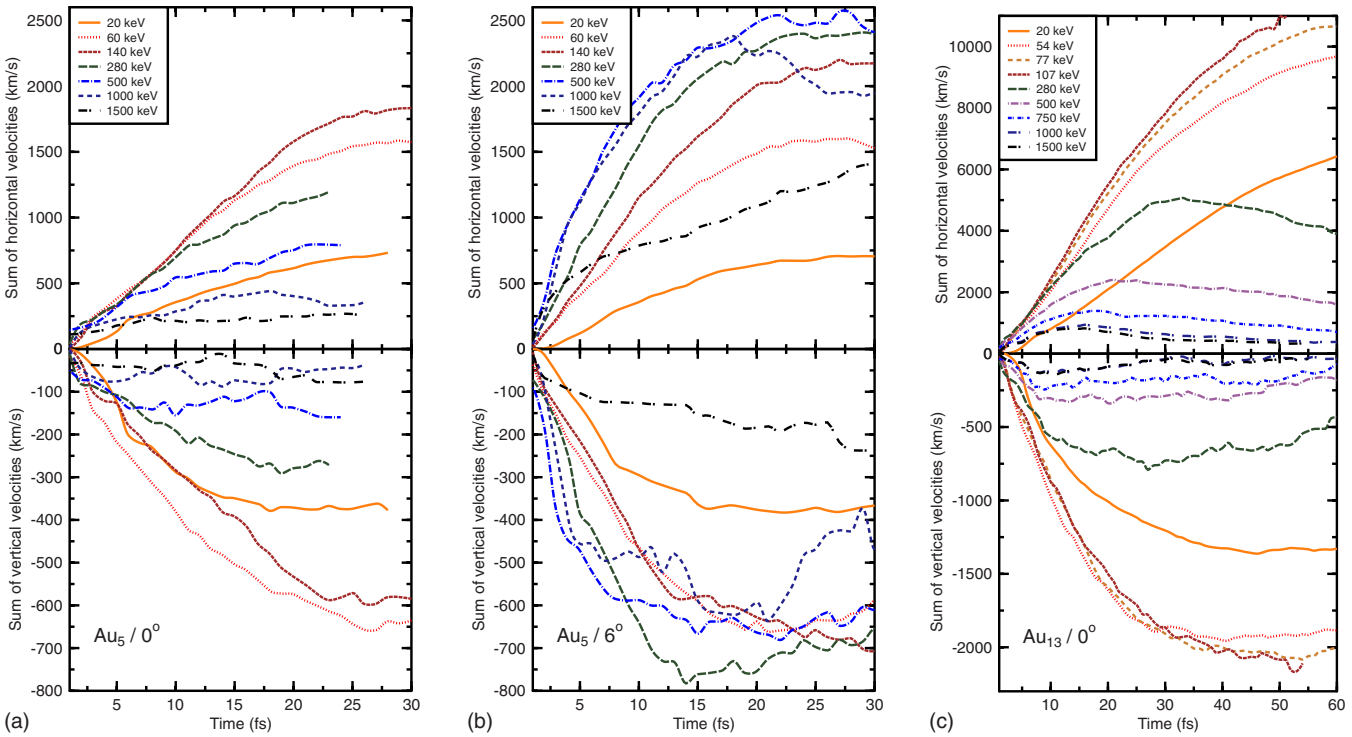

FIG. 6. (Color online) Sums of horizontal and vertical velocities (total momenta) of the crystal atoms located in a rectangular volume ($4\times4\times14$ nm^3) surrounding the cluster track. Notice the different velocity scale in the Au_{13} results. The horizontal velocity is defined as the sum of absolute values of atomic velocities parallel to the surface. The vertical velocity is the component perpendicular to the surface. The velocities of the cluster atoms are not included in the summation.

either, because the energy is transmitted elsewhere to the crystal by the fast knock-on atoms and these collisions do not occur near each other. Finally, the collisions depositing relatively small energies and occurring close to each other induce dense displacement cascades.[27,28]

An important quantity in this process is the mean free path between displacement collisions. For single Au ion bombardment of a Au target, the mean free path of the primary knock-on atoms can be approximated with the following formula:[27]

$$\lambda_d \approx 0.000\,12 \frac{E_i\sqrt{E_c}}{\sqrt{E_i} - \sqrt{E_c}}. \quad (1)$$

E_i is the energy of the ion and E_c the energy gained by the knock-on atom. When $E_i \gg E_c$, we can approximate that $\lambda_d \propto \sqrt{E_i E_c}$. At $E_c = 10$ keV, the free path increases from 5 to 16 nm when the ion energy increases from 60 to 1500 keV. Therefore, the probability that the displacement collisions of knock-on atoms form a dense network around the cluster track decreases with E_c.

To test the assumption that only particular collisions contribute to cascade formation, we sorted the collisions according to their energy and filtered out channeling collisions and high-energy collisions. The results are shown in Fig. 8. A collision is considered as a channeling collision if $E_i > 50$ keV, $E_c < 20$ keV, and $\delta v_h < 50$ km/s, where δv_h is the

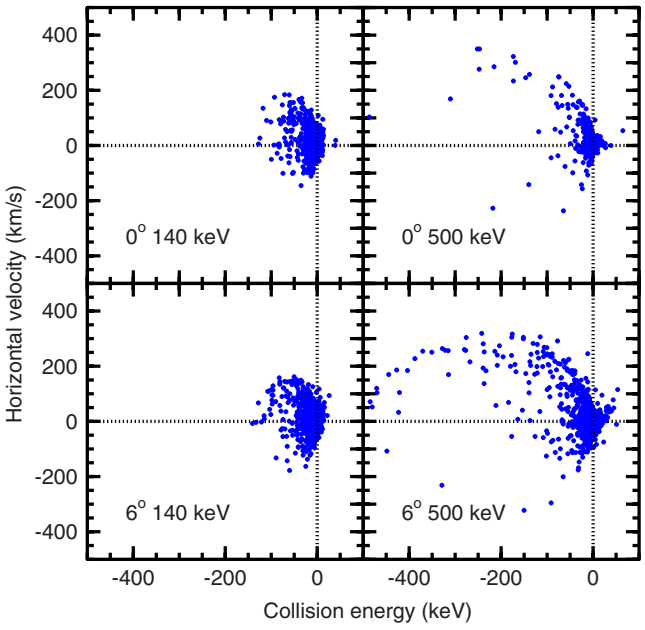

FIG. 7. (Color online) Correlation of energies and horizontal velocities transferred in Au_5 collision events. Each frame shows results from 32 runs. The negative energy values indicate that in some collisions, the cluster atoms gain energy from other cluster atoms either directly or transmitted by the crystal atoms.

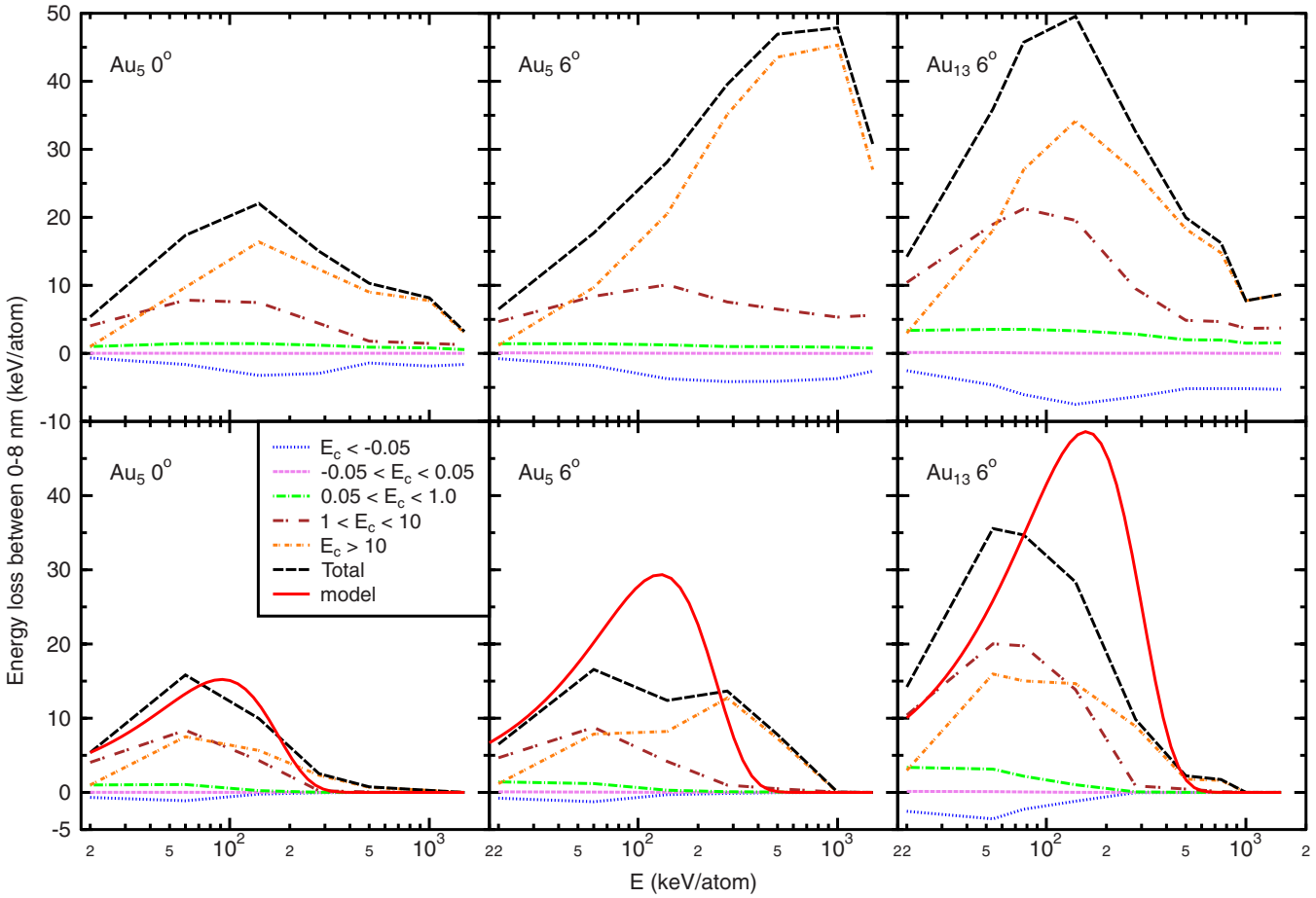

FIG. 8. (Color online) Cluster energy loss in the 8 nm deep surface layer divided in components coming from collisions of different strengths. The energy E_c gained by the knock-on atoms in the collision is used to classify the collisions in the strength categories. The upper frames show the original energy losses and the lower frames the losses after filtering the collision events. The functional forms fitted in the yield distributions (Fig. 1) are shown in the lower frames (continuous lines) for comparison to the total energy loss curve.

change of the horizontal velocity. The high-energy collisions are defined to have $\sqrt{E_i E_c} > 70$ keV. This limit is somewhat artificial, because there is no clear energy limit for the collisions inducing cascades. The contribution of very weak collisions that exchange energy less than a typical displacement energy, that is, 44 eV for Au,[27] is negligible.

The filtered energies correspond to the sputtering yields (Fig. 8). For comparison, the functions listed in Table I are plotted against the energy curves scaling them linearly. The portion of energy contributing to the cascade formation can be called *damage energy*.

TABLE I. Parameter values of function $Y = CN^2 E_i \exp(-BE_i^2)$ [Eq. (4)] fitted to the experimental and simulated data (Fig. 1).

Cluster	Angle (deg)	C (keV^{-1})	B (keV^{-2})
Au_5 expt.	0	0.9±0.1	$(0.9\pm0.2)\times10^{-5}$
Au_5	0	3.5±0.5	$(6.0\pm2.0)\times10^{-5}$
Au_5	6	3.5±1.0	$(3.0\pm1.0)\times10^{-5}$
Au_{13}	0	1.4±0.4	$(2.0\pm2.0)\times10^{-5}$

F. Cascade expansion

Figure 9 shows how a typical 280 keV/atom cascade develops to a full crater gradually. At 100 fs, the cascade has started to develop and subcascades induced by departed cluster atoms and fast knock-on atoms are shown. The width of the cascade is around 40 nm.

The expansion goes on until the cascade has reached its full size at around 1 ps. From this and other visualizations, it is clearly seen that during the expansion, the knock-on atoms first induce subcascades leaving crystal structure untouched between them. Later, the structure collapses because of the expansion of the subcascades. This leapfrogging continues until the energy density of the frontier is too weak to displace atoms. The jumps of knock-on atoms are shorter than 1 nm, indicating that the primary high-energy knock-on atoms are not contributing according to Eq. (1).

After that, the cascade still expands because of melting of the border regions and especially because the pressure inside the cascade pushes the borders further. Pressure induced coherent displacements are clearly seen in Fig. 9. The release of the pressure and sputtering mechanisms are discussed in a related article.[13]

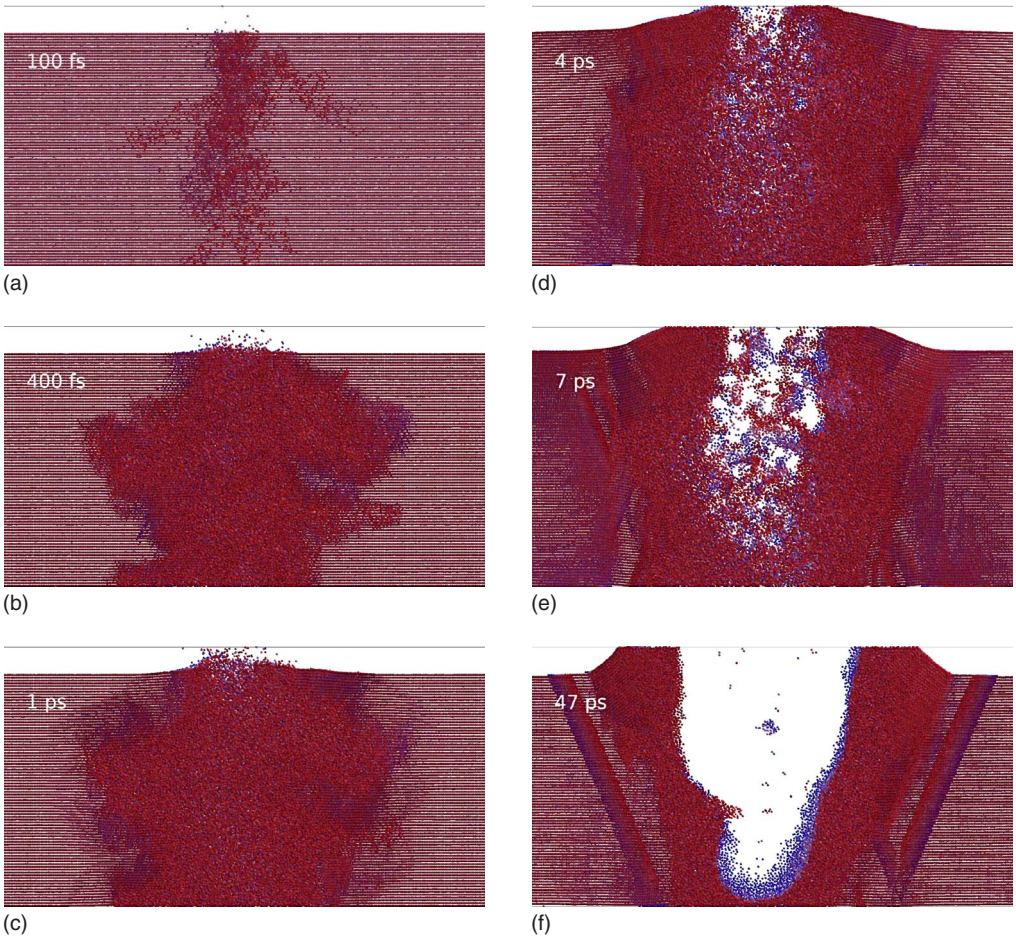

FIG. 9. (Color online) Visualization of cascade development after an impact of 280 keV Au_5. Times of snapshot from left to right and from top to bottom are 100 fs, 400 fs, 1 ps, 4 ps, and 47 ps. The frames show $4 \times 22 \times 2$ nm^3 slices; thus, the bottom in each frame is located at 20 nm from the surface. The stripes shown around the crater in the 47 ps frame are coherent displacements induced by the lateral pressure (Ref. 29).

IV. DISCUSSION

A. Droplet form

We now introduce a mathematical model that describes the average energy deposition in cluster collisions and predicts the sputtering yield. The model is based on the average form of collision cascade observed in the simulations, which is a consequence of the cascade development mechanisms discussed in the previous sections. The model has an interesting geometrical interpretation, which leads us to call it the droplet model. At small angles of incidence, the displacement cascades have, in average, a droplet form that emerges from the atomic level processes of cluster energy deposition and cascade development. Examples of the form are shown in Fig. 10.

Bombardment of gold crystals in molecular dynamics simulations with gold clusters of different nuclearities and energies shows that the collision cascade inside the crystal has a rather regular form and size when the cluster has more than a few atoms. The form of the cluster collision cascade depends on nuclearity and energy of the cluster, the main characteristics being the following. Low-energy clusters stop onto the surface, which is called cluster deposition. More energetic clusters, e.g., 10 keV/atom Au_5, produce a collision cascade beneath the surface that has the form of a hemisphere. High-energy clusters ($E > 100$ keV/atom Au_5) first penetrate inside the crystal lattice as a whole leaving a track of energetic atoms behind them. Let us call this cylindrical track the tail. When a high-energy cluster is slowed down enough, it gradually falls apart and forms an ellipsoidal collision cascade inside the solid. At very high energies, the cascade is almost like a thin cylinder.

The droplet shape consists of a half ellipsoid and a tail as shown in Fig. 10. As the cluster energy increases, the cluster penetrates deeper into the crystal and both the droplet tail and ellipsoid become longer. The intersection area A of a droplet tail and a crystal surface can be calculated by describing the profile of the tail with the Gaussian function

$$A = \pi(Re^{-L^2})^2, \tag{2}$$

where R is the radius of the intersection and L is the length of the tail. L can be interpreted to be the depth of the thickest part of the cascade where the most damaging energy release has occurred (Fig. 10). The simulations indicate that the tail

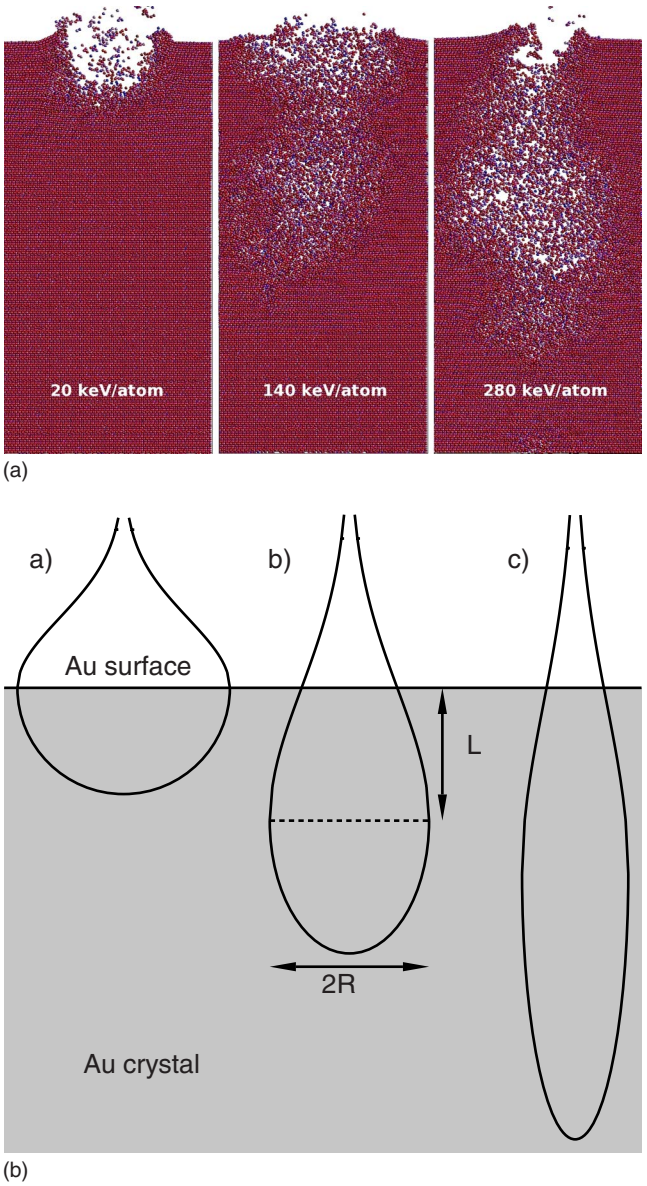

FIG. 10. (Color online) Left: Examples of simulated collision cascades of Au_5 clusters. Each figure shows a 0.5 nm thick and 16 nm wide slice of the crystal 1.5–3.0 ps after the collision. At this stage, the cluster has broken apart and its energy is deposited to the secondary atoms, which has moved away from the initial collision region. Right: Schematic figure of the droplet model. Sputtering yield depends on the intersection area of the surface and the droplet shape, which describes the average shape of collision cascades. The portions of the imaginary droplets inside the solid have variable shapes depending on energy, and the cross section area varies. At low energies (a), the shape is almost perfect hemisphere, and at high energies (c), the shape is almost a cylinder. Between these extremes, a droplet shape appears (b).

is relatively independent of nuclearity because of the channeling. So, L grows with channeling.

On the other hand, the sputtering yield Y is approximately linearly proportional to the crater area, although it is a sum of yields caused by different sputtering mechanisms.[13] Thus, the sputtering yield and the form of the cascade are related.

B. Origin of the droplet form

The cluster track through the 5–10 mm surface layer is initially less than 1 mm wide cylinder perpendicular to the surface. Immediately after the cluster has passed a layer, the track consists of primary knock-on atoms that have different energies and directions depending on types of collisions. The knock-on atoms jump out from the track to distances according to the mean free paths defined in Eq. (1) starting to form a displacement cascade. Because the track is cylindrical, we can reduce the problem to two dimensions and consider jumps and displacements of knock-on atoms only in layers parallel to the surface.

The average damage energy E_d induced in a surface layer by each cluster atom is approximately

$$E_d \propto E_i \exp(-BE_i^2), \tag{3}$$

where E_i is the energy of the cluster atom and B is a parameter. The exponent function describes the probability of cascade inducing collisions at the surface. This particular functional form is chosen because of the droplet form discussed in the previous section. It is a damping factor that sums up all effects that either decrease the energy deposition, like channeling, or decrease the damage accumulation in the vicinity of the initial track, like long jumps of high-energy knock-on atoms.

If we approximate that Eq. (1) is valid also for secondary knock-on atoms, then both the primary and secondary jump lengths are approximately proportional to $\sqrt{E_d}$. In other words, the longer the jump, the larger the subcascade it induces. If the subcascades overlap, a uniform displacement region formed. Otherwise, the subcascades remain separated by crystalline regions. This has two consequences.

(1) If the number of primary knock-on atoms is doubled, the cascade will be twice as wide as the original. The geometrical reasoning leading this assumption is explained in the Appendix.

(2) The diameter of the cascade grows also proportional to $\sqrt{E_d}$.

The knock-on process continues until the energy of the displaced atoms is not high enough to induce more displacements. The expansion of the cascade can be roughly described as a process of discrete steps where, at each step, a cylindrical cascade sends knock-on atoms radially out from its surface and these atoms form subcascades which, in turn, form a new layer of displacements around the original cascade. The diameter of the cascade is proportional to $N\sqrt{E_d}$, where N is the cluster nuclearity (number of atoms in the cluster). It is assumed that the cascades induced by the cluster atoms develop independently and the radius of the unified cascade increases linearly with the number of cluster atoms.

The sputtering yield Y is linearly proportional to the crater area.[13] On the other hand, the crater diameter is about the same as the cascade diameter, as shown in Fig. 9. Thus $Y \propto (N\sqrt{E_d})^2$. If we substitute Eq. (1) to this relation, we get an empirical formula for the sputtering yield,

$$Y = CN^2 E_i \exp(-BE_i^2), \quad (4)$$

where B and C are adjustable parameters. Y/N^2 does not depend on nuclearity, as Bouneau *et al.* have observed with a polycrystalline target.[6]

Equation (4) is a good approximation even when the final phases of the expansion of the cascade are strengthened by the pressure inside the cascade, because the pressure inside the cylindrical cascade is proportional to the diameter. This is based on the observation that the atoms move, on average, toward the surface of the cascade, leaving a void region in the center (Fig. 9). So, the displacement cascade is not a classical gas container where the gas has a homogeneous density.

C. Validity of the model

The model is valid for clusters coming at 0°–6° angle of incidence so that the cluster atoms relatively easily go into the channels perpendicular to the surface. Larger angle of incidence or grain boundaries in polycrystalline targets distort the droplet form and a more complicated mathematical formulation is required. However, the basic energy deposition and cascade development processes are the same.

The experimental Au_5 yield from a polycrystalline target has its maximum at considerable higher energy than the simulated yields from Au(111). According to the model, this is a consequence of lower probability of channeling. In a polycrystalline target, the yield is an average of yields from microcrystals with various orientations. Because Au(111) has relatively low channeling probability, the yield from a polycrystalline target should rather have its maximum lower at the energy scale than the yield from Au(111). Thus, the lower channeling probability should have an explanation that is based on some other properties of polycrystalline targets. A possible explanation is the higher collision probability at grain boundaries. The finer grains in the target, the higher is the probability that the cluster hits a close neighborhood of a grain boundary. The cluster atoms or the primary knock-on atoms have to cross the boundary when they pass the surface layer. This increases the number of displacement collisions and decreases the channeling probability. Test simulations confirm this qualitatively.

Equation (4) is fitted to the yield data (Fig. 1), and the resulting parameter values are listed in Table I. In the model, the parameter B defines the place of maximum yield and describes the probability of channeling and the other factors decreasing the cascade formation. Its value depends on the angle of incidence as the Au_5 simulations show. The value is larger at normal incidence, and the maximum yield is reached at lower energy than at 6°.

B has the same value within uncertainty in the normal incidence Au_5 and Au_{13} cases, which means that the maximum yield is reached at the same energy. This is one requirement for the observation of the N^2 effect, because the experimental sputtering yields Y/N^2 of clusters of different sizes have their maxima at the same energy.[6] On the other hand, the parameter C does not have the same value in the Au_5 and Au_{13} cases, which is an indication that the N^2 is not reproduced. However, neither experimental nor simulated Au_{13} data are available at high energies, and it is not possible to make a conclusion whether or not the N^2 effect is really reproduced in these simulations. It is also possible that the effect is characteristic for the polycrystalline targets, but in single crystal targets, the parameters B and C depend on nuclearity.

Shao *et al.* has developed a model for cluster induced displacement cascades based on the same idea of overlapping cascades of the cluster atoms,[30] but the mathematical formulation of their model is different than ours. They conclude that the overlap mechanism provides an adequate description for cluster induced cascades, and their model can predict how the damaged region in silicon grows with Au cluster size. This result supports our conclusion that the overlapping cascades of the cluster atoms are the main reason for the nonlinear effects in cluster impacts. On the other hand, the analysis of the collision mechanisms presented in the previous sections provides explanations on how the cluster atoms deposit their energy and how their overlapping cascades finally form the large displacement region.

The droplet model shows that at least the main features of the cascade development can be explained without considering special coherent interactions of the cluster atoms when they move through the material or coherent effects such as Coulomb explosion in the cascade.[31–34] In the interaction model used in the simulations, the attractive interatomic forces depend solely on the approximated electronic density induced by the neighbor atoms without any excitations or electronic correlation effects. The short distance repulsive forces are calculated using the ZBL approximation,[14] which describes single ion collisions with a target. However, there is experimental evidence that the nuclear stopping power of an atom in a cluster is less than the nuclear stopping of a single ion,[35] probably due to the sheltering effect. Interactions between closely moving cluster atoms, known as vicinage effects, introduce even more complicated interactions than the sheltering effect, and these effects are under discussion.[34,36–38]

The droplet model is based on several approximations which are valid in target elements similar to gold. In many respects, the model is very general and we suppose it is valid for all dense materials, which do not have structure that distorts collision cascades spatially.

V. CONCLUSIONS

Energy deposition during the first femtoseconds in nanocluster impacts is analyzed using molecular dynamics. It is shown that the sputtering yield is not directly proportional to the energy deposited from the clusters in the surface layers, especially at high energies. Most of the energy deposited in high-energy head-to-head collisions does not contribute to displacement cascade formation, which decreases the sputtering yield. In addition, a cluster can channel through the surface layers as one entity undergoing no violent collisions with the crystal atoms.

A model that gives the average sputtering yield as function of the cluster energy is given. The model demonstrates that the energy dependence of cluster induced sputtering

yields can be, to a great extent, explained considering the effective damage energy deposited from the cluster and assuming that the first phases of the displacement cascade expansion are dominated by jumps of knock-on atoms. The model can explain the N^2 effect and an energy maximum that differs from the nuclear stopping. However, it cannot reproduce the highest-energy tail of the experimental data, which is most likely due to differences in sample structure.

The model also demonstrates that the atomic level processes, which are building blocks of the model, can be reasonably simulated with molecular dynamics, which is an application of classical equations of motion and where the interactions are modeled with rather approximative interatomic potentials. Therefore, we conclude that the most dominant features of cluster collisions and sputtering in fcc metals can be explained without reference to coherent phenomena such as Coulomb explosion or coherent quantum states inside the cascade.

ACKNOWLEDGMENTS

We thank E. M. Bringa and K. O. E. Henriksson for useful discussions. This work was performed within the Finnish Centre of Excellence in Computational Molecular Science (CMS), financed by The Academy of Finland and the University of Helsinki. Generous grants of computer time from the Center for Scientific Computing in Espoo, Finland are gratefully acknowledged.

APPENDIX: SUBCASCADE OVERLAPPING

Let R be the distance that a knock-on atom moves from its initial position before it collides with a lattice atom and let r be the radius of the subcascade it induces. If both R and r are linearly proportional to $\sqrt{E}$, where E is the energy of the knock-on atom, then $r \propto R$.

Let us assume that n knock-on atoms are induced in a cluster track approximately at the same depth, they all have the same energy, and they spread horizontally. Because they have the same energy, they induce subcascades at a circle of radius R. The cascades begin to overlap if the sum of their diameters is equal to the circumference of the circle and if the subcascades are located at regular intervals. Let θ be the angle between the tracks of two knock-on atoms. Then, the cascades begin to overlap if

$$r \cos(\theta/2) = R \sin(\theta/2). \tag{A1}$$

Because $r \propto R$, the condition for the overlapping does not depend on energy of the knock-on atoms. Instead, the overlapping occurs if θ is small enough; in other words, enough knock-on atoms are induced. If the first cluster atom induces a number of knock-on atoms that are enough to cover only half of the circumference, then two cluster atoms induce enough knock-on atoms to cover the circumference. Thus, doubling the number of cluster atoms doubles the radius of the final cascade.

*juha.samela@helsinki.fi

[1] V. N. Popok and E. E. B. Campbell, Rev. Adv. Mater. Sci. **11**, 19 (2006).
[2] P. Sigmund and C. Clausen, J. Appl. Phys. **52**, 990 (1981).
[3] A. V. Samartsev, A. Duvenbeck, and A. Wucher, Phys. Rev. B **72**, 115417 (2005).
[4] H. H. Andersen and H. L. Bay, J. Appl. Phys. **45**, 953 (1974).
[5] H. H. Andersen, A. Brunelle, S. Della-Negra, J. Depauw, D. Jacquet, Y. LeBeyec, J. Chaumont, and H. Bernas, Phys. Rev. Lett. **80**, 5433 (1998).
[6] S. Bouneau, A. Brunelle, S. Della-Negra, J. Depauw, D. Jacquet, Y. LeBeyec, M. Pautrat, M. Fallavier, J. C. Poizat, and H. H. Andersen, Phys. Rev. B **65**, 144106 (2002).
[7] D. Jacquet and Y. L. Beyec, Nucl. Instrum. Methods Phys. Res. B **193**, 227 (2002).
[8] S. Zimmermann and H. B. Urbassek, Nucl. Instrum. Methods Phys. Res. B **228**, 75 (2005).
[9] S. Zimmermann and H. M. Urbassek, Nucl. Instrum. Methods Phys. Res. B **255**, 208 (2007).
[10] E. Salonen, K. Nordlund, and J. Keinonen, Nucl. Instrum. Methods Phys. Res. B **212**, 286 (2003).
[11] K. Nordlund, J. Keinonen, M. Ghaly, and R. S. Averback, Nature (London) **398**, 49 (1999).
[12] K. O. E. Henriksson, K. Nordlund, and J. Keinonen, Phys. Rev. B **71**, 014117 (2005).
[13] J. Samela and K. Nordlund, Nucl. Instrum. Methods Phys. Res. B (to be published).
[14] J. F. Ziegler, J. P. Biersack, and U. Littmark, *The Stopping and Range of Ions in Matter* (Pergamon, New York, 1985).
[15] K. Nordlund, Comput. Mater. Sci. **3**, 448 (1995).
[16] A. Duvenbeck, F. Sroubek, Z. Sroubek, and A. Wucher, Nucl. Instrum. Methods Phys. Res. B **225**, 464 (2004).
[17] J. D. Kress and A. E. DePristo, J. Chem. Phys. **88**, 2596 (1988).
[18] C. L. Kelchner, D. M. Halstead, N. M. W. L. S. Perkins, and A. E. DePristo, Surf. Sci. **310**, 425 (1994).
[19] H. Hakkinen, M. Moseler, and U. Landman, Phys. Rev. Lett. **89**, 033401 (2002).
[20] J. Samela, J. Kotakoski, K. Nordlund, and J. Keinonen, Nucl. Instrum. Methods Phys. Res. B **239**, 331 (2005).
[21] K. Nordlund, M. Ghaly, R. S. Averback, M. Caturla, T. Diaz dela Rubia, and J. Tarus, Phys. Rev. B **57**, 7556 (1998).
[22] M. Ghaly, K. Nordlund, and R. S. Averback, Philos. Mag. A **79**, 765 (1999).
[23] T. J. Colla, H. M. Urbassek, A. Wucher, C. Staudt, R. Heinrich, B. J. Garrison, C. D., and G. Betz, Nucl. Instrum. Methods Phys. Res. B **143**, 284 (1998).
[24] Nucl. Instrum. Methods Phys. Res. B **83**, 73 (1993).
[25] I. Baranov, S. Della-Negra, M. Fallavier, S. Kirillov, Y. L. Beyec, A. Novikov, V. Obnorskii, K. Wien, and S. Yarmiychuk, Nucl. Instrum. Methods Phys. Res. B **245**, 184 (2006).
[26] K. Nordlund, Comput. Mater. Sci. **3**, 448 (1995).
[27] M. Nastasi, J. W. Mayer, and J. K. Hirvonen, *Ion-Solid Interactions* (Cambridge University Press, Cambridge, England, 1996).
[28] F. Rossi, D. M. Parkin, and M. Nastasi, J. Mater. Res. **14**, 137

(1989).
[29] K. Nordlund, J. Keinonen, M. Ghaly, and R. S. Averback, Nucl. Instrum. Methods Phys. Res. B **148**, 74 (1999).
[30] L. Shao, M. Nastasi, X. Wang, J. Liu, and W.-K. Chu, Nucl. Instrum. Methods Phys. Res. B **242**, 503 (2006).
[31] E. Nardi, Z. Zinamon, T. A. Tombrello, and N. M. Tanushev, Phys. Rev. A **66**, 013201 (2002).
[32] Z. L. Miskovic, W.-K. Liu, and Y.-N. Wang, Phys. Rev. A **57**, 362 (1998).
[33] Z. L. Miskovic, W.-K. Liu, and Y.-N. Wang, Phys. Rev. A **58**, 2191 (1998).
[34] H.-W. Li, Y.-N. Wang, and Z. L. Miskovic, J. Phys.: Condens. Matter **16**, 1231 (2004).
[35] H. H. Andersen, A. Johansen, M. Olsen, and V. Touboltsev, Nucl. Instrum. Methods Phys. Res. B **212**, 56 (2003).
[36] N. R. Arista, Nucl. Instrum. Methods Phys. Res. B **164**, 108 (2000).
[37] S. A. Cruz, E. G. Gamaly, L. T. Chadderton, and D. Fink, Radiat. Meas. **36**, 145 (2003).
[38] Z. L. Miskovic, T. L. Wilson, and Y.-N. Wang, Phys. Rev. A **67**, 022903 (2003).